

Black Carbon Emissions from Associated Natural Gas Flaring

Cheryl L. Weyant,^{*,†} Paul B. Shepson,[‡] R. Subramanian,[§] Maria O. L. Cambaliza,^{||} Alexie Heimburger,[‡] David McCabe,[⊥] Ellen Baum,[#] Brian H. Stirn,[∇] and Tami C. Bond[†]

[†]Civil and Environmental Engineering, University of Illinois Urbana–Champaign, Urbana, Illinois 61801, United States

[‡]Department of Chemistry, Purdue University, West Lafayette, Indiana 47907, United States

[§]Department of Mechanical Engineering, Carnegie Mellon University, Pittsburgh, Pennsylvania 15213, United States

^{||}Department of Physics, Ateneo de Manila University, Quezon City, Philippines

[⊥]Clean Air Task Force, Boston, Massachusetts 02108, United States

[#]Climate and Health Research Network, Bowdoinham, Maine 04008, United States

[∇]School of Aviation & Transportation Technology, Purdue University, West Lafayette, Indiana 47907, United States

S Supporting Information

ABSTRACT: Approximately 150 billion cubic meters (BCM) of natural gas is flared and vented in the world annually, emitting greenhouse gases and other pollutants with no energy benefit. About 7 BCM per year is flared in the United States, and half is from North Dakota alone. There are few emission measurements from associated gas flares and limited black carbon (BC) emission factors have been previously reported from the field. Emission plumes from 26 individual flares in the Bakken formation in North Dakota were sampled. Methane, carbon dioxide, and BC were measured simultaneously, allowing the calculation of BC mass emission factors using the carbon balance method. Particle optical absorption was measured using a three-wavelength particle soot absorption photometer (PSAP) and BC particle number and mass concentrations were measured with a single particle soot photometer. The BC emission factors varied over 2 orders of magnitude, with an average and uncertainty range of 0.14 ± 0.12 g/kg hydrocarbons in associated gas and a median of 0.07 g/kg which represents a lower bound on these measurements. An estimation of the BC emission factor derived from PSAP absorption provides an upper bound at 3.1 g/kg. These results are lower than previous estimations and laboratory measurements. The BC mass absorption cross section was 16 ± 12 m²/g BC at 530 nm. The average absorption Ångström exponent was 1.2 ± 0.8 , suggesting that most of the light absorbing aerosol measured was black carbon and the contribution of light absorbing organic carbon was small.



■ INTRODUCTION

Petroleum deposits often have a gaseous component, commonly called “associated gas”, that consists of methane and other short chain hydrocarbons. Associated gas extracted as a byproduct of oil production may be flared or vented if it is not collected or used on-site.

One hundred and forty to one hundred and seventy billion standard cubic meters (BCM) of associated gas is flared and vented in the world annually.^{1,2} The United States contributes about 7 BCM per year and about half of that is from North Dakota.³ The volume of natural gas flared in North Dakota increased from 0.09 BCM in 2004 to 3.7 BCM in 2014, a 40-fold increase in 10 years.⁴ Horizontal drilling and high-volume hydraulic fracturing has led to increased oil production in the Bakken region, North Dakota. However, production wells have preceded the development of gas transportation pipelines, so a significant fraction of the gas produced is flared. About 30% of

the gas produced in the Bakken was flared in 2014, down from a peak of almost 50% in 2008, although the magnitude of flaring has increased in that time period. In comparison, the rest of the U.S. flares less than 1% of associated gas.³

From a global warming perspective, flaring is preferable to venting. Flaring oxidizes carbon and creates CO₂, but reduces the overall global warming potential of the emissions by destroying methane and other hydrocarbons. Fossil methane is 36 times more potent than CO₂ on a 100 year time-scale.^{5–7} Flaring reduces emissions of flammable global warming gases, but also creates other pollutants, such as NO_x, CO, and black carbon (BC).

Received: September 25, 2015

Revised: January 7, 2016

Accepted: January 14, 2016

Published: January 14, 2016

Black carbon is a combustion byproduct that contributes to climate warming. BC absorbs solar radiation in the atmosphere, influences cloud dynamics, and darkens ice surfaces and accelerates melting. Including all known forcing mechanisms, the current atmospheric radiative forcing of BC is estimated to be $+1.1$ ($+1.0/-0.93$) Wm^{-2} , relative to preindustrial values.⁸ BC radiative forcing is second only to CO_2 , which contributes 1.68 (± 0.35) Wm^{-2} .⁶

The GAINS global emission inventory estimates that flaring emits 4% of global BC emissions, at 230 Gg yr^{-1} , a factor of 3 greater than on-road gasoline vehicles (80 Gg yr^{-1}).^{8,9} The global emissions are relatively small, yet due to emissions at high latitude, associated gas flares were modeled to be the source of 42% of BC surface concentrations in the Arctic atmosphere, where BC-induced ice melting is hypothesized to occur.⁵

The BC emission factor, the mass of BC emitted relative to the quantity of gas flared, is an important metric that facilitates estimations of emissions from the industry. There are no published field measurements of BC emission factors from individual associated gas flares. Field and laboratory emission testing of flares have reported combustion efficiency or destruction efficiency of fuel components.^{10–13} Ground-based optical measurements have been used to estimate BC emission rates from gas flares in the field,^{14–16} but emission factors were not reported in these studies. Schwarz et al. (2015)¹⁷ conducted aircraft sampling in the Bakken and determined an average BC emission factor from the region that included BC from flares and other sources, but they did not sample individual flares. Laboratory studies that measure turbulent diffusion flames have found that fuel gases and flame turbulence affect emission factors,^{18–20} so variability in individual emission factors is likely.

None of these studies estimate BC emissions from flares as operated, and field studies evaluate either one or two flares or an average over an entire region. As a complement to these studies that describes the emission behavior of individual flares, this study reports measurements of BC emission factors from individual associated gas flares. Individual gas flares were sampled using both laser-induced incandescence and absorption-based BC measurements to provide lower and upper bounds, respectively, on emission factors. Flare emissions were measured in the Bakken region, North Dakota, in March 2014.

MATERIALS AND METHODS

Measurements of BC, CO_2 , and CH_4 were conducted for 26 gas flares in the Bakken formation, North Dakota using aircraft sampling. The sampling campaign included 85 flight passes through flare plumes in nine flights in March 2014. Individual flares were sampled with 1–6 flight passes, and two flares were sampled on multiple days. Each flight was limited by the fuel and was about 5 h. The Purdue University's Airborne Laboratory for Atmospheric Research (ALAR), a Beechcraft Duchess aircraft, flew into the plume from downwind. This small aircraft was instrumented for wind and chemical species measurements, and can fly relatively slowly (45 m/s) to enable adequate sampling in a small plume.

Flares were sighted from the aircraft and then selected for sampling. Both ground flares and elevated stack flares were sampled and were distinguished by observation. Fuel composition, instantaneous gas flow rates, and details about flare designs were not known for the sites measured. However, the monthly volume of gas flared in March 2014 was known for

some of the well sites⁴ and an estimation of average gas composition in the Bakken formation was available.²¹

Aircraft and Instrumentation. The aircraft was equipped with a Best Air Turbulence (BAT) probe for wind measurements, a global positioning and inertial navigation system (GPS/INS), and a microbead thermistor.^{22,23} The BAT probe is a nine-port pressure differential probe that extended from the nose of the aircraft. It measured and recorded wind speed and wind direction at 50 Hz. The measured pressure variations across the hemisphere of the probe were combined with 50 Hz inertial data from GPS/INS to obtain three-dimensional wind vectors.

Ambient air was drawn into the nose of the aircraft and through 5 cm diameter PTFE Teflon tubing at a flow rate of 1840 L min^{-1} using a high-capacity blower located at the rear of the aircraft. The sampled gases were drawn into three sampling instruments from this central duct. There was a 20% particle loss in the sampling system (including the inlet probe, duct and sample line) as determined from ground measurements at sampling flow rates. The particle loss was not a strong function of particle size for the particle sizes measured ($25\text{--}150 \text{ nm}$). The sampling inlet was subisokinetic (duct velocity was about 18 m/s and the plane was traveling at about 45 m/s at the time of sampling). There would be an enhancement of particle sampling efficiency of 25% for particles of $0.1 \mu\text{m}$ diameter.

A cavity ring-down spectrometry system (CRDS, model G2301-m, Picarro Inc.) was used for in situ, real-time measurements of CO_2 , CH_4 , and H_2O . The CRDS system measured gas concentrations at 0.5 Hz at a flow rate of 850 mL min^{-1} . The aircraft was equipped with an in-flight calibration system for CH_4 and CO_2 , using two NOAA/ESRL reference cylinders (cylinder 1: 1785.85 nmol/mol and $377.857 \mu\text{mol/mol}$ and cylinder 2: 2656.83 nmol/mol and $441.898 \mu\text{mol/mol}$ for CH_4 and CO_2 , respectively). The measurement precision for CO_2 and CH_4 have routinely and consistently been found to be 0.05% and 0.1%, respectively, and comparisons to NOAA whole air samples support accuracies of 0.2% and 0.1%, respectively, corresponding to $\pm 0.9 \text{ ppm}$ for CO_2 and 3 ppb for CH_4 .

Two aerosol instruments were on-board the aircraft, a Single Particle Soot Photometer (SP2, Droplet Measurement Technologies)^{24–26} and a three wavelength Particle Soot Absorption Photometer (PSAP, Radiance Research). The SP2 measures laser-induced incandescence of refractory BC-containing aerosols. The incandescence signal is proportional to BC mass and this relationship was determined in laboratory calibrations using fullerene soot. The SP2 was used to determine black carbon mass in individual particles, including those internally mixed with other materials.^{27,28} Only particles with a mass of BC greater than 0.7 fg are detected with 100% efficiency.²⁹ Although some particles were below this threshold, less than 5% of the mass was undetected because the larger particles contribute more to the BC mass. In addition, coincident particle detection can cause undersampling of 5–10% of the BC mass. Primary SP2 data were analyzed as in Subramanian et al. (2010) and then resolved at 1 Hz for further analysis.³⁰ Leading edge scattering signals have been used to predict scattering from BC particle coatings that are vaporized in normal instrument use,³¹ but the SP2 in this study was not configured for this analysis. The BC particle size ranged from $0.005\text{--}0.8 \mu\text{m}$ with a mass median diameter of $0.22 \mu\text{m}$ and is not significantly different than the $0.188 \mu\text{m}$ found in Schwarz et al. (2015).¹⁷ Further details about the SP2 calibration,

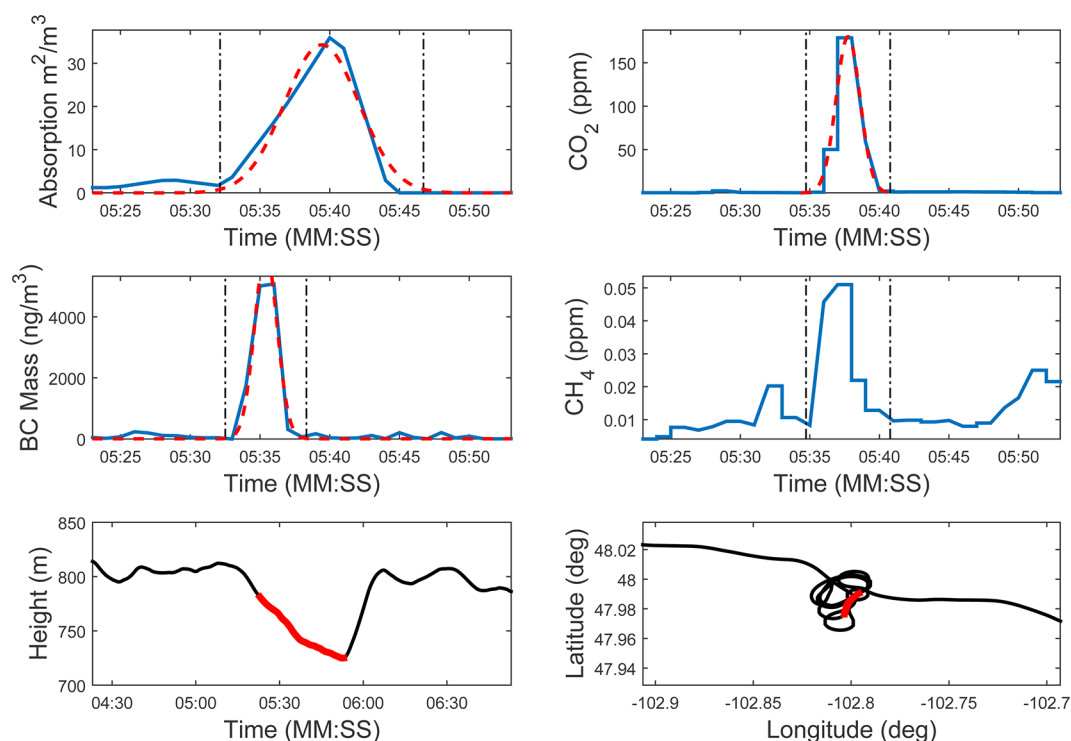


Figure 1. Measurements taken during a single flare pass. The real-time data is shown in blue for the four signals: particle absorption from the PSAP (top left), CO_2 (top right), CH_4 (middle right), and the BC mass from the SP2 (middle left). Gaussian peak fits are shown as dashed red lines. The vertical black dashed lines show the width of the integration periods. The bottom left and right plots show the height and location of the of the aircraft at the time of sampling. The red portion identifies the time period shown in the real-time plots.

coincidence analysis, and BC coating thickness estimation can be found in the [Supporting Information \(SI\)](#).

The PSAP continuously detects light absorption by particles at 467, 530, and 660 nm on a filter, including absorption by non-BC particles. Absorption at each wavelength was recorded every four seconds. Filter transmittance was maintained in the acceptable range of 0.5–1.0 throughout the entire sampling campaign. The flow through the instrument was measured with a primary flow calibrator (mini-BUCK Calibrator M-5, A. P. BUCK, INC.) before and after every day of sampling and was used to calibrate an internal real-time flow sensor. The PSAP signal was corrected for flow rate, spot size, and adjusted to atmospheric pressure³² and a loading-dependent correction was applied.

The study design included both SP2 and PSAP measurements to provide constraints on emission factors given uncertainties inherent in each technique. The SP2 is expected to underestimate emission factors because it does not detect the smallest BC particles and is subject to saturation in high concentrations. On the other hand, the SP2 can be used to analyze particle-level details. The PSAP can only capture integral absorption over the entire plume and is not exclusively selective for BC absorption. However, the PSAP does not have the same size and saturation constraints as the SP2. Both instruments produced good results; the SP2 shows little bias due to missing particles and the PSAP is not strongly influenced by non-BC absorption. The paired data are thus useful to calculate another important characteristic of emissions: the mass absorption cross-section, which is required in order to infer the radiative effect of black carbon.

Data Analysis. Emission factors (in grams BC per kg associated gas) were calculated using the ratio of BC mass to

the total carbon mass measured in each flare pass. Emissions were also reported in grams BC per volume associated gas using gas composition data from the Bakken (see [SI Table 1](#)). This carbon balance method is typical for emission factor calculations for combustion emissions,^{33–35} especially for sources without stacks. Carbon, above background and measured as CO_2 , CH_4 , and BC, in the plume was assumed to be entirely from the combustion of associated gas, so that the mass of excess carbon in the plume was equal to the mass of carbon from the fuel. This calculation assumes that emissions of other carbon-containing species are negligible. Carbon monoxide and other hydrocarbon emissions are assumed to be zero in this analysis. The CO/CO_2 ratio in a laboratory flare has been measured as less than 0.002,³⁶ suggesting that CO forms a negligible fraction of carbon.

For each species, the carbon balance calculation requires the concentration of excess carbon in the plume, which is obtained by subtracting background from plume concentrations. Background concentrations were determined by assigning the lowest 10th percentile of each full flight data set as background. While this cutoff value is arbitrary, use of the 70th percentile would decrease the BC emission factors by less than 5% and the mass absorption cross sections by less than 4%.

Each signal peak was integrated to determine the amount of pollutant captured in a single pass. The aircraft typically sampled the flare plume for about two seconds, but due to the different response times and sampling rates of the instruments, the peaks they generated ranged from 3 to 10 s. Alignment of the signals for a point-by-point analysis, as in the gas-phase measurements of Caulton et al. (2014),¹¹ was not feasible. For each signal separately, 20 seconds of data around each peak was run through a bootstrapping routine that minimized the

residuals between a Gaussian fit and the data, and identified a Gaussian curve that best fit the data³⁷ (Figure 1). The width of the Gaussian peak was used to determine the integration period for each signal. An exception was CH₄, which was measured with the same instrument as CO₂. Methane can be emitted from leaks on the well pad in addition to the flare. An assumption was made that CH₄ within the CO₂ peak originated from the flare plume itself, while CH₄ outside that peak came from leaks. This assumption was implemented by integrating CH₄ over the same time period as the CO₂ peak.

Passes for which the maximum CO₂ peak was greater than 10 times the standard deviation of the background (10 σ) above the average background were included in the data set. When BC mass, aerosol absorption, or CH₄ were below the detection limit (3 σ above background), they were assigned a value of half the detection limit for the emission factor calculation. Other combustion emission sources may be present near the flare, including vehicle emissions, diesel engines, and small flares on storage tanks. The contributions from these unquantified sources may appear in both the background and in the plume. The 10 σ cutoff identifies flare plumes sampled that are clearly elevated above background. Only five passes were omitted due to this constraint. Two were small flares and for three, the flight was too far from the source.

The emission factor for BC was determined using eq 1.

$$EF_{BC} = 1000F \frac{C_{BC}}{C_{CO_2} + C_{CH_4} + C_{BC}} \quad (1)$$

C_{BC} , C_{CO_2} , and C_{CH_4} are mass concentrations of carbon in each species in g/m³ and F is the carbon mass fraction of the gas in grams carbon per grams of hydrocarbons in the fuel gas. The carbon content of the fuel was not measured, but has little variation (0.77–0.75) over a wide range of fuel mixtures (see SI Table 1). A value of 0.77 was used, which is based on reported gas composition in the Bakken.²¹ Associated gas can contain significant amounts of inert gases such as N₂, CO₂ or He. The emission factors given here are in grams BC per kg of hydrocarbons in associated gas, which connects emission measurements to a quantity that is easily measured and closely connected to energy content of the flared gas. Any CO₂ present in the fuel gas would bias BC emission factors low. Associated gas in the Bakken typically contains less than 1% CO₂²¹ (see SI Table 1).

The mass absorption cross-section of BC (MAC_{BC} in m²/g BC) is the ratio of the absorption coefficient (b) in m⁻¹ (m²/m³) to C_{BC} and indicates the strength of the absorption per mass of BC in m²/g BC. The absorption Ångström exponent (AAE) is a measure of the wavelength dependence of the absorption. AAE values of about 1 are typical for graphitic carbon, whereas values of 3.5–7 are found for light absorbing organic aerosols.⁸ Here, AAE is determined between the 467 and 660 nm wavelengths using eq 2.

$$AAE = -\frac{\ln(b_{660}/b_{467})}{\ln(660/467)} \quad (2)$$

Reported mass absorption cross-section and AAE do not include values in the denominator below the detection limit.

RESULTS AND DISCUSSION

Black Carbon Absorption. The magnitude of BC mass peaks was strongly correlated with the magnitude of the

absorption peaks for all passes ($R^2 = 0.89$), suggesting consistency in the absorption of the BC emitted from this source. The average and standard deviation of the mass absorption cross-section of BC for all the passes was 22 ± 16 , 16 ± 12 , and 14 ± 10 m²/g BC at 467, 530, and 660 nm wavelengths, respectively. A histogram of MAC_{BC} (530 nm) showing all flare passes is shown in Figure 2. MAC_{BC} at 530 nm for individual passes ranged from 3.1–41 m²/g BC, and the median was 16 m²/g BC at 530 nm.

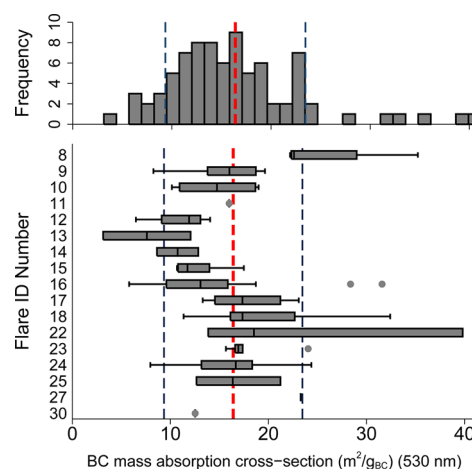


Figure 2. Distribution of MAC_{BC} at 530 nm. Top: histogram of all passes through a flare plume. The average and uncertainty range for all passes was 16 ± 12 m²/g BC and are shown in the figure as the red and blue dashed, vertical lines. The box and whisker plot shows the range of MAC_{BC} for each flare. The centerline of each box is the median, the box represents the 25th through 75th percentile, the whiskers represent the most extreme value within 1.5 times the interquartile range, and the points beyond the whiskers are values outside this range.

A typical value for MAC_{BC} for pure BC is 7.5 ± 1.2 m²/g BC at 550 nm,^{8,38} about half the median value found here. This high value of MAC_{BC} is not fully explained. However, many sources, including flares, were not included in the assessment of MAC_{BC} in Bond and Bergstrom (2006), and 7.5 m²/g BC does not represent a conclusive value from all sources. Absorption of BC can be enhanced when BC particles are coated with non-BC aerosol components, such as water or organic material.²⁸ However, the relative humidity in the plume was low in these experiments ($48 \pm 25\%$) so the presence of condensed water is unlikely. Some condensation of heavy hydrocarbons onto BC particles is possible. If the associated gas contained 0.08 g condensable hydrocarbons per gram methane,²¹ at environmental temperatures, sufficient heavy hydrocarbons (3 g condensable hydrocarbons per gram BC) could condense on the BC to increase the absorption by a factor of 1.4 (see SI).³⁹ The SP2 did not detect the mass in very small particles, an underestimation that would make the measured MAC_{BC} higher than the true value. Additional absorption by non-BC material can occur but is not consistent with these measurements as shown in the next section or the coating thickness analysis in the SP2 (see SI).

If the absorption measurements, along with a typical MAC_{BC} of 7.5 m²/g BC are used to approximate the BC mass, the resulting BC mass emission factors would be 2.2 times higher than measured by the SP2. This possible increase represents an upper bound on the emission factors in this study.

Absorption Ångström exponent. The average AAE measured for all the flare passes was 1.2 ± 0.8 (Figure 3).

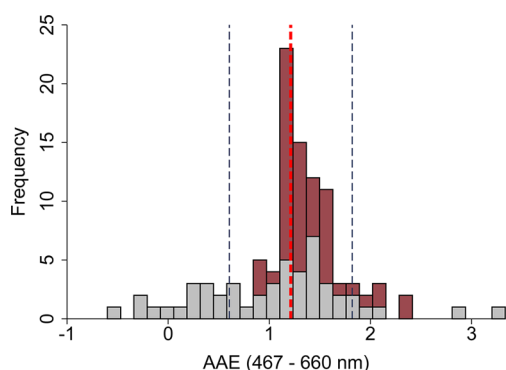


Figure 3. Histogram of the absorption Ångström exponent (AAE) between the 467 and 660 nm. The gray bars show flare passes with low levels of absorption (below $100 \text{ m}^{-1}\text{s}$ integrated absorption) and the maroon bars are passes above this threshold. The vertical lines represent the mean and uncertainty range (1.2 ± 0.8).

There was greater variability in passes with low absorption (below $100 \text{ m}^{-1}\text{s}$ integrated peak). For low absorption measurements, AAE ranged from -0.6 to 3.3 , and for high absorption the AAE was 0.9 to 2.3 . However, this variability does not affect the average, which was 1.4 ± 0.33 when low absorption peaks are excluded. This result suggests that most of the light absorbing aerosol measured is black carbon and the contribution of organic carbon is small. Using the method suggested in Lack et al. (2013), and assuming the AAE of pure BC is 1, an estimated eight percent of the absorption is predicted to be from non-BC absorbing aerosols. However, the contribution of non-BC aerosol is not statistically different from zero.⁴⁰ AAE is uncorrelated with MAC_{BC} , suggesting that organic carbon does not affect the MAC_{BC} .

Black Carbon Emission Factor. Figure 4 shows the distribution of BC emission factors for all the passes, including a separation by individual flare. Black carbon emission factors ranged over 2 orders of magnitude. The average BC emission factor was 140 mg/kg hydrocarbons in associated gas with an uncertainty range of 120 mg/kg and a median of 68 mg/kg (median absolute deviation: 53 mg/kg). Several observations were above 500 mg/kg and the histogram of all the BC emission factors is right-skewed.

Average BC emission factors for individual flares varied from 2.3 to 330 mg/kg associated gas. Individual flares can be grouped into three statistically different categories: low, medium, and high emitters, with averages of 5.0 , 53 , and 270 mg/kg ($p < 0.01$). This suggests that there are differences in combustion conditions or gas composition that cause variability in BC emission factors. Emission factors from ground flares ($74 \pm 46 \text{ mg/kg}$ gas, $n = 7$) were smaller than stack flares (200 ± 280 , $n = 64$), but the difference was not statistically significant ($p > 0.1$).

Explanations for the large variability in the BC emission factor were sought. Environmental factors measured were not predictive; the BC emission factor was not correlated ($r < 0.4$, $p = 0.05$) with the ambient temperature, pressure, or humidity. High wind speeds at the time of sampling could increase the turbulence of the flames and influence particle emissions, but wind speed was not correlated with BC mass emission factor ($R^2 = 0.02$), although the range of wind speed during sampling

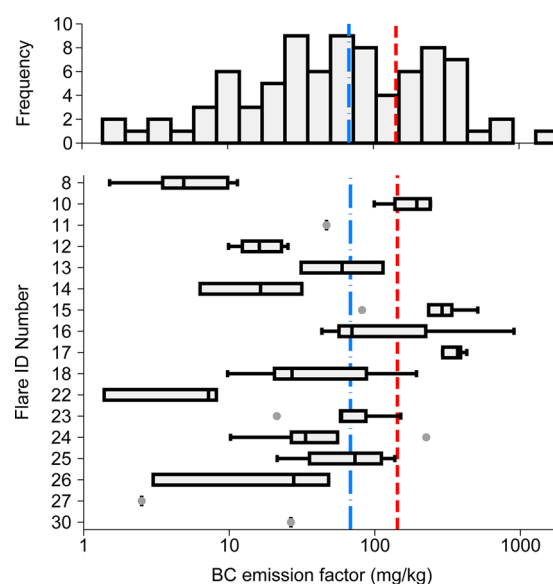


Figure 4. Histogram of black carbon emission factors (mg/kg associated gas) for all passes and a box and whisker plot grouped by individual flare. Both panels use the same data and are on a log scale. The box and whisker plots are calculated as in Figure 2. The red dashed lines represent the mean and the blue dash-dot lines represent the median of all of the passes.

was low ($3.5\text{--}6 \text{ m/s}$). Caulton et al. (2014) reported a correlation of methane emission factor with wind speed, but over a much greater range ($5\text{--}15 \text{ m/s}$).¹¹ Elevated methane in the plume could imply a lower combustion efficiency, which is sometimes correlated with BC emissions. However, CH_4 and BC mass emissions were not correlated ($R^2 < 0.01$). A relationship between the BC emission factor and the reported volume of gas flared per month at the well pad was investigated. The monthly volume of gas flared was available for a subset of the measured flares and varied by 2 orders of magnitude ($1500\text{--}108\,000 \text{ m}^3/\text{month}$). BC emission factors tended to be higher and more variable at wells with greater flare volumes, but the correlation was weak ($R^2 = 0.1$, SI Figure S1).

The two flares that were resampled on different days did not maintain consistent BC emission factors. In one flare (#16), BC emission factors on different days were statistically different ($p < 0.1$) with values of 57 , 699 , and 64 mg/kg . Emission factors were in the high range for 1 out of 3 days of sampling and in the low range on the other two. Another flare (#18) also had different emission factors on two separate days ($p < 0.01$) and were in the medium group on 1 day and the low group on the other. Variability in BC emission factors may be influenced by gas flow rates and gas composition, which can vary from day to day. This information is not available for the flares in this study.

Implications. BC emission factors measured in this study are lower than previous measurements and estimates. The average emission factor in the study, using the SP2 measurements, is $0.14 \pm 0.12 \text{ g/kg}$ associated gas, or $0.13 \pm 0.36 \text{ g/m}^3$, assuming a gas density of $0.9 \pm 0.2 \text{ kg/m}^3$ (SI Table 1). If the absorption measurements are used to predict an emission factor instead of the SP2, an upper bound on the emission factor would be 0.31 g/kg associated gas (0.28 g/m^3). Laboratory measurements of flares with specific composition in Becker et al. (1982) gave 1.12 g/kg for pure methane fuel and higher values for heavier hydrocarbons.¹⁸ McEwen et al. (2012) measured emission factors in flares with fuel mixtures typical in

the oil and gas industry and found an average emission factor of 0.74 g/kg,²⁰ six times higher than the average found in this study. Schwarz et al. (2015) measured an upper bound emission factor of 0.57 ± 0.14 g/m³ from flares in the Bakken, and is consistent with the lower emission factors measured here.¹⁷ Stohl et al. (2013) used an estimated BC emission factor of 1.6 g/m³ to calculate an emission inventory, reasoning that field emissions would be higher than laboratory measurements.⁹ The Canadian Association of Petroleum Producers reports 2.5632 g PM/m³,⁴¹ based on measurements of PM from a landfill flare, where composition is expected to contain lighter hydrocarbons on average. The U.S. Environmental Protection Agency compendium of emission factors lists values for PM concentrations in exhaust gases from flares from a study of refinery flares which are not representative of associated gas flaring.⁴²

If the emission factors measured in this study are representative spatially and temporally, then flaring from the Bakken formation emits approximately 0.36 Gg BC per year. Global emissions of BC would be 20 ± 6 Gg BC per year, assuming a global flared volume of 155 ± 15 billion cubic meters and the emission factors measured here. This estimate for the flaring contribution to the global BC burden is 11 times lower than the 228 Gg-BC/year given in Stohl et al. (2013).⁹ This magnitude of global flaring emissions would be similar to that of other low-BC emitting sectors, such as global aviation and power plant emissions of BC (20 Gg BC).⁸ In contrast, BC emissions from diesel engines are 2 orders of magnitude higher (1300 Gg BC).⁸

These emission values provide an estimate of the global BC emissions from associated gas flares, given the available data. However, BC emission factors from flares in other regions, including Russia, which dominates global emissions from flaring,¹ may have substantially different emission factors and characteristics. In addition, none of the flares measured in this study had visible, high-density smoke. Visibly smoking flares have been described in the literature^{43,44} suggesting that the highest emitters may not have been captured. The measurements reported here characterize emission quantities and properties from flares without visible smoke.

■ ASSOCIATED CONTENT

● Supporting Information

The Supporting Information is available free of charge on the ACS Publications website at DOI: 10.1021/acs.est.5b04712.

Gas composition used for analysis and additional BC coating methods are shown in Supporting Information (PDF)

■ AUTHOR INFORMATION

Corresponding Author

*Phone: (217) 333-6967; fax: (217) 333-0687; e-mail: weyant@illinois.edu.

Notes

The authors declare no competing financial interest.

■ ACKNOWLEDGMENTS

We thank Amara Holder for providing SP2 coincidence code, Joel Rindelaub for particle loss measurements, and Kerri Pratt for assessment of the inlet efficiency. This work was funded by the Clean Air Task Force.

■ REFERENCES

- (1) Elvidge, C. D.; Ziskin, D.; Baugh, K. E.; Tuttle, B. T.; Ghosh, T.; Pack, D. W.; Erwin, E. H.; Zhizhin, M. A fifteen year record of global natural gas flaring derived from satellite data. *Energies* **2009**, *2*, 595–622.
- (2) Elvidge, C. D.; Zhizhin, M.; Hsu, F.-C.; Baugh, K. E. VIIRS nightfire: Satellite pyrometry at night. *Remote Sensing* **2013**, *5*, 4423–4449.
- (3) U.S. Energy Information Administration, Natural Gas Gross Withdrawals and Production. http://www.eia.gov/dnav/ng/ng_prod_sum_a_epg0_vgv_mmcf_a.htm (accessed March 23, 2015).
- (4) North Dakota Industrial Commission, Department of Mineral Resources, Oil and Gas Division, Historical monthly gas production and sales statistics. <https://www.dmr.nd.gov/oilgas/stats/statisticsvw.asp> (accessed February 18, 2015).
- (5) Holmes, C. D.; Prather, M. J.; Søvdø, O.; Myhre, G. Future methane, hydroxyl, and their uncertainties: key climate and emission parameters for future predictions. *Atmos. Chem. Phys.* **2013**, *13*, 285–302.
- (6) Myhre, G.; Shindell, D.; Brèon, F.; Collins, W.; Fuglestedt, J.; Huang, J.; Koch, D.; Lamarque, J.; Lee, D.; Mendoza, B.; Nakajima, T.; Robock, A.; Stephens, G.; Takemura, T.; Zhang, H. *Anthropogenic and Natural Radiative Forcing. Climate Change 2013: The Physical Science Basis. Contribution of Working Group I to the Fifth Assessment Report of the Intergovernmental Panel on Climate Change*; Cambridge University Press, Cambridge, 2013.
- (7) Boucher, O.; Friedlingstein, P.; Collins, B.; Shine, K. P. The indirect global warming potential and global temperature change potential due to methane oxidation. *Environ. Res. Lett.* **2009**, *4*, 044007.
- (8) Bond, T.; et al. Bounding the role of black carbon in the climate system: A scientific assessment. *Journal of Geophysical Research D: Atmospheres* **2013**, *118*, 5380–5552.
- (9) Stohl, A.; Klimont, Z.; Eckhardt, S.; Kupiainen, K.; Shevchenko, V.; Kopeikin, V.; Novigatsky, A. Black carbon in the Arctic: The underestimated role of gas flaring and residential combustion emissions. *Atmos. Chem. Phys.* **2013**, *13*, 8833–8855.
- (10) Pohl, J. H.; Tichenor, B. A.; Lee, J.; Payne, R. Combustion efficiency of flares. *Combust. Sci. Technol.* **1986**, *50*, 217–231.
- (11) Caulton, D. R.; Shepson, P. B.; Cambaliza, M. O.; McCabe, D.; Baum, E.; Stirr, B. H. Methane destruction efficiency of natural gas flares associated with shale formation wells. *Environ. Sci. Technol.* **2014**, *48*, 9548–9554.
- (12) Stroscher, M. T. Characterization of emissions from diffusion flare systems. *J. Air Waste Manage. Assoc.* **2000**, *50*, 1723–1733.
- (13) Torres, V. M.; Herndon, S.; Kodesh, Z.; Allen, D. T. Industrial flare performance at low flow conditions. I. Study overview. *Ind. Eng. Chem. Res.* **2012**, *51*, 12559–12568.
- (14) Johnson, M. R.; Devillers, R. W.; Yang, C.; Thomson, K. A. Sky-scattered solar radiation based plume transmissivity measurement to quantify soot emissions from flares. *Environ. Sci. Technol.* **2010**, *44*, 8196–8202.
- (15) Johnson, M. R.; Devillers, R. W.; Thomson, K. A. Quantitative field measurement of soot emission from a large gas flare using Sky-LOSA. *Environ. Sci. Technol.* **2010**, *45*, 345–350.
- (16) Johnson, M.; Devillers, R.; Thomson, K. A generalized Sky-LOSA method to quantify soot/black carbon emission rates in atmospheric plumes of gas flares. *Aerosol Sci. Technol.* **2013**, *47*, 1017–1029.
- (17) Schwarz, J. P.; Holloway, J. S.; Katich, J. M.; McKeen, S.; Kort, E.; Smith, M. L.; Ryerson, T.; Sweeney, C.; Peischl, J. Black carbon emissions from the Bakken oil and gas development region. *Environ. Sci. Technol. Lett.* **2015**, *2*, 281–285.
- (18) Becker, H.; Liang, D. Total emission of soot and thermal radiation by free turbulent diffusion flames. *Combust. Flame* **1982**, *44*, 305–318.
- (19) Sivathanu, Y.; Faeth, G. M. Soot volume fractions in the overfire region of turbulent diffusion flames. *Combust. Flame* **1990**, *81*, 133–149.

- (20) McEwen, J. D.; Johnson, M. R. Black carbon particulate matter emission factors for buoyancy-driven associated gas flares. *J. Air Waste Manage. Assoc.* **2012**, *62*, 307–321.
- (21) Wocken, C. A.; Stevens, B. G.; Almlie, J. C.; Schlasner, S. M. End-of-use technology study: An assessment of alternative uses of associated gas. In *Topical Report for North Dakota Industrial Commission*, Contract No. G024-052, 2012.
- (22) Crawford, T. L.; Dobosy, R. J. A sensitive fast-response probe to measure turbulence and heat flux from any airplane. *Boundary-Layer Meteorology* **1992**, *59*, 257–278.
- (23) Garman, K.; Hill, K.; Wyss, P.; Carlsen, M.; Zimmerman, J.; Stirm, B.; Carney, T.; Santini, R.; Shepson, P. An airborne and wind tunnel evaluation of a wind turbulence measurement system for aircraft-based flux measurements. *Journal of Atmospheric and Oceanic Technology* **2006**, *23*, 1696–1708.
- (24) Stephens, M.; Turner, N.; Sandberg, J. Particle identification by laser-induced incandescence in a solid-state laser cavity. *Appl. Opt.* **2003**, *42*, 3726–3736.
- (25) Baumgardner, D.; Kok, G.; Raga, G. Warming of the Arctic lower stratosphere by light absorbing particles. *Geophys. Res. Lett.* **2004**, *31*.[10.1029/2003GL018883](https://doi.org/10.1029/2003GL018883)
- (26) Schwarz, J.; Gao, R.; Fahey, D.; Thomson, D.; Watts, L.; Wilson, J.; Reeves, J.; Darbeheshti, M.; Baumgardner, D.; Kok, G. Single-particle measurements of midlatitude black carbon and light-scattering aerosols from the boundary layer to the lower stratosphere. *J. Geophys. Res., Atmos. (1984–2012)* **2006**, *111*.
- (27) Moteki, N.; Kondo, Y. Effects of mixing state on black carbon measurements by laser-induced incandescence. *Aerosol Sci. Technol.* **2007**, *41*, 398–417.
- (28) Cross, E. S.; Onasch, T. B.; Ahern, A.; Wrobel, W.; Slowik, J. G.; Olfert, J.; Lack, D. A.; Massoli, P.; Cappa, C. D.; Schwarz, J. P. Soot particle studies-instrument inter-comparison-project overview. *Aerosol Sci. Technol.* **2010**, *44*, 592–611.
- (29) Schwarz, J.; Spackman, J.; Gao, R.; Perring, A.; Cross, E.; Onasch, T.; Ahern, A.; Wrobel, W.; Davidovits, P.; Olfert, J. The detection efficiency of the single particle soot photometer. *Aerosol Sci. Technol.* **2010**, *44*, 612–628.
- (30) Subramanian, R.; Kok, G.; Baumgardner, D.; Clarke, A.; Shinozuka, Y.; Campos, T.; Heizer, C.; Stephens, B.; De Foy, B.; Voss, P. Black carbon over Mexico: the effect of atmospheric transport on mixing state, mass absorption cross-section, and BC/CO ratios. *Atmos. Chem. Phys.* **2010**, *10*, 219–237.
- (31) Gao, R.; Schwarz, J.; Kelly, K.; Fahey, D.; Watts, L.; Thompson, T.; Spackman, J.; Slowik, J.; Cross, E.; Han, J.-H. A novel method for estimating light-scattering properties of soot aerosols using a modified single-particle soot photometer. *Aerosol Sci. Technol.* **2007**, *41*, 125–135.
- (32) Bond, T. C.; Anderson, T. L.; Campbell, D. Calibration and intercomparison of filter-based measurements of visible light absorption by aerosols. *Aerosol Sci. Technol.* **1999**, *30*, 582–600.
- (33) Akagi, S.; Yokelson, R. J.; Wiedinmyer, C.; Alvarado, M.; Reid, J.; Karl, T.; Crouse, J.; Wennberg, P. Emission factors for open and domestic biomass burning for use in atmospheric models. *Atmos. Chem. Phys.* **2011**, *11*, 4039–4072.
- (34) Laursen, K. K.; Ferek, R. J.; Hobbs, P. V.; Rasmussen, R. A. Emission factors for particles, elemental carbon, and trace gases from the Kuwait oil fires. *J. Geophys. Res.* **1992**, *97*, 14491–14497.
- (35) Herndon, S. C.; Nelson, D. D., Jr; Wood, E. C.; Knighton, W. B.; Kolb, C. E.; Kodosh, Z.; Torres, V. M.; Allen, D. T. Application of the carbon balance method to flare emissions characteristics. *Ind. Eng. Chem. Res.* **2012**, *51*, 12577–12585.
- (36) Poudenx, P. Plume sampling of a flare in crosswind: Structure and combustion efficiency, M.Sc. Thesis, University of Alberta, Edmonton, AB. 2000.
- (37) O'Haver, T. Command-line peak fitting program for time-series signals, MATLAB Central File Exchange. <http://www.mathworks.com/matlabcentral/fileexchange/23611-command-line-peak-fitting-program-for-time-series-signals>.
- (38) Bond, T. C.; Bergstrom, R. W. Light absorption by carbonaceous particles: An investigative review. *Aerosol Sci. Technol.* **2006**, *40*, 27–67.
- (39) Bond, T. C.; Habib, G.; Bergstrom, R. W. Limitations in the enhancement of visible light absorption due to mixing state. *J. Geophys. Res.* **2006**, *111*.[10.1029/2006JD007315](https://doi.org/10.1029/2006JD007315)
- (40) Lack, D.; Langridge, J. On the attribution of black and brown carbon light absorption using the Ångström exponent. *Atmos. Chem. Phys.* **2013**, *13*, 10535–10543.
- (41) Canadian Association of Petroleum Producers. *NPRI Guide - A Recommended Approach to Completing the National Pollutant Release Inventory for the Upstream Oil and Gas Industry*, 2014.
- (42) McDaniel, M.; Tichenor, B. A. *Flare Efficiency Study*, 1983.
- (43) Ite, A. E.; Ibok, U. J. Gas flaring and venting associated with petroleum exploration and production in the Nigeria's Niger Delta. *American Journal of Environmental Protection* **2013**, *1*, 70–77.
- (44) Aghalino, S. Gas flaring, environmental pollution and abatement measures in Nigeria, 1969–2001. *Journal of Sustainable Development in Africa* **2009**, *11*, 219–238.